P121 Preliminary Results of a U.S. Deep South Warm Season Deep Convective Initiation Modeling Experiment using NASA SPoRT Initialization Datasets for Operational National Weather Service Local Model Runs

Jeffrey M. Medlin[1], Lance Wood[2], Bradley Zavodsky[3] Jonathan L. Case[4] and Andrew Molthan[3]

[1]NOAA National Weather Service; Mobile, AL
[2]NOAA National Weather Service (NWS); Houston, TX
[3]NASA Short-term Prediction Research and Transition (SPoRT) Center/Marshall Space Flight Center; Huntsville, Alabama
[4] NASA SPoRT Center/ENSCO, Inc.; Huntsville, Alabama

1. INTRODUCTION

Warm season deep convective initiation remains a difficult forecast challenge in the relative high thermodynamic instability and low deep-layer vertical wind shear environment of the U.S. Deep South. Our overall understanding of the link between readily observable coastal mesoscale circulations (e.g., sea-, bay- and land-breezes) that initiate deep convection has improved over recent decades but still falls well short of fully describing the seemingly random nature of first initiate locations along such prominent features. Owing to the fact that boundary layer moisture flux convergence cannot be observed or forecast on the scale of locally developing cumuli, the problem becomes even more complicated over inland areas where subtle surface boundaries can easily go undetected by modern day remote sensing for a variety of reasons

On the scale of developing cumuli, local variations in surface conditions due to soil moisture and type, vegetation and land-water thermal contrasts strongly influence the resultant fluxes that directly affect the location and timing of deep convective initiation. A mesoscale model being run at convection allowing resolutions (i.e. without use of a convective parameterization scheme; e.g., Kain et al. 2010) can exploit real-time remotely-sensed data sets which yield information regarding prevailing initial conditions within the surface layer. This is considered to be a ripe area for operational research and development.

A joint collaborative modeling effort between the National Weather Service (NWS) Offices in Mobile, AL (MOB) and Houston, TX (HGX) and the National Aeronautics and Space Administration's (NASA) Short-term Prediction Research and Transition Center (SPoRT) was undertaken during the 2012 warm season to examine the effects of utilizing certain NASA Products within the NOAA/NWS Science and Training Resource Center (STRC) Environmental Modeling System (EMS; Rozumalski 2012). These products include: 3-km Land Information System (LIS) land surface data, 2-km SPoRT blended sea surface temperature and green vegetation fraction (GVF) composites derived from Moderate Resolution Imaging Spectroradiometer (MODIS) on a Continental U.S. domain with 1-km grid spacing.

Collectively, each product has been shown through similar separate studies to add value to mesoscale model forecasts (LaCasse et al. 2008 [SST]; Case et al. 2008 [LIS]; Case et al. 2011 [LIS+SST]; and Case et al. 2012 [MODIS GVF]). This paper describes the preliminary results of the project through a couple of cases highlighting the impact of the aforementioned data sets and finally presents preliminary

*****_Corresponding author address_: Jeffrey Medlin, NWS Mobile, AL, 8400 Airport Blvd., Bldg. #11, Mobile, AL 36608. Email: jeff.medlin@noaa.gov

objective verification results between an operational run (OPL, with NASA data sets) and a control run (CTL; without).

2. PROJECT DESIGN

Using the National Center for Atmospheric Research (NCAR) Advanced Research WRF (ARW) dynamical core, two EMS domains with identical physical settings were established over the southeast Texas and Alabama coastlines. The model was initialized at 0600 UTC each day to mitigate the cold start problem with regard to precipitation and was run out to 24 h with a 54 s time step using the full resolution GFS personal tiles (0.205° native grid) as both the initial and boundary conditions. The model was run at 9-km resolution and possesses a 3 km one-way inner nest. The Kain-Fritsch convective parameterization scheme was employed on the outer domain; no convective parameterization was used on the inner nest. The model configuration employs the WRF Single-Moment 6-Class microphysics scheme, the Mellor-Yamada-Janjic boundary layer mixing scheme and the RRTM (longwave radiation) and Dudhia (shortwave radiation) schemes, respectively (details of these physics parameterization schemes are found in Skamarock et al. 2008). The OPL runs (i.e., those including the NASA data sets) were the operational forecasts generated daily by each WFO; the NASA SPoRT Center ran the CTL. However, after a test revealed the existence of non-linear variations in model solutions due to computational platform differences, it was decided that for the purpose of removing these biases from the final evaluation that both the HGX and MOB OPL runs as well as the CTL would be run at the NASA SPoRT Center (see Section 3).

The Model Evaluation Tools (MET; Brown et al. 2009) package was used to compute both point and grid statistics comparing the operational and control forecasts. Hourly Stage IV precipitation accumulations on the 5-km grid from the Hydrologic Rainfall Analysis Project (HRAP) were used to perform gridded precipitation verification. For both 2-m temperature and dewpoint temperature and 10-m wind verification, hourly Meteorological Assimilation Data and Ingest System (MADIS) point data were used.

3. COMPUTATIONAL PLATFORM DIFFERENCES DUE TO NON-LINEAR VARIATIONS

The non-linear processes in mesoscale models require floating-point precision and are sensitive to how a computational platform handles the floating-point calculations. Previous sensitivity simulations conducted at the National Severe Storms Laboratory have shown that convective placement can be displaced by as much as one county (~30 km) simply due to the different handling of floating point calculations on disparate computational platforms, compilers, and/or operating systems (Kain, personal communication). In light of their findings, SPoRT, HGX, and MOB personnel felt it prudent to test the degree to which these differences are manifested in the modeling configurations and different computational platforms herein.

Sensitivity simulations conducted on the SPoRT vs. MOB, and SPoRT vs. HGX platforms confirmed there were indeed visual differences in the simulated reflectivity. Figure 1 shows a comparison of two 13-hour forecasts of simulated composite reflectivity run independently on SPoRT and MOB's computational platforms. The model setup was identical and the only variable was the differing computational platforms. The difference field between the two reveals results that could lead to different interpretations and also show that in order for meaningful verification to be performed, both the CTL and OPL runs must be carried out on the same platform. Although not shown, similar results were found for HGX's domain for an independent, separate case day. To remove this issue, SPoRT performed re-runs of the operational EMS for candidate warm season convective initiation days (i.e. nominal synoptic forcing). The operational cases could then be optimally compared to the control runs, which were also run on the same platform by SPoRT.

4. CONVECTIVE INITIATION CASES

Two individual case study examples (one from each model domain) are presented below. The first case from 3 July 2012 highlights the impact of the MODIS GVFs while the second case from 28 June 2012 highlights the issue of precipitation underestimation that was a common observation during this study in both model domains.

4.1 *3 July 2012 Central Gulf Coast Case Study*

3 July 2012 was one of the first case days that significant deep convection was initiated subsequent to a regional ‘mini-drought’ period from 12 June to 2 July 2012. Despite having one of the wettest summers on record along portions of the Central Gulf Coast, the area temporarily came under the influence of the U.S. Plains deeply-reflected large scale ridge whose subsidence suppressed rainfall for many months leading into the Summer of 2012. In early June and prior to the occurrence of the regional ‘mini-drought’, a record rainfall occurred along the coastal areas of Alabama and the western Florida Panhandle (see Fig 2., and note the northwest to southeast gradient in rainfall that exists from eastern MS to the western FL Panhandle). Figure 3 shows the GVF difference field [OPL-CTL], which indicates more ‘greenness’ versus climatology in areas that experienced record rainfall versus much drier areas over eastern MS. Unlike the real-time SPoRT/MODIS product, the climatology GVF cannot account for vegetation responses to weather and climate anomalies such as rainfall surpluses, deficits, or prolonged temperature departures, each of which can impact the health and coverage of vegetation. A more representative depiction of GVF can in turn improve the partitioning of net radiation into sensible, latent, and ground heat fluxes in land surface models, thereby improving boundary layer processes that can lead to the initiation of deep, moist convection.

Figure 4 depicts 88D Level II 0.5° radar reflectivity values ≥35 dBZ valid simultaneous with a 12-h forecast of 950 hPa moisture flux convergence for the CTL versus the OPL runs, respectively. Note the relatively stronger pattern of moisture flux convergence produced by the model along the coast for the operational run versus that of the control. Presumably, a more realistic representation of the near-surface vegetation, in turn, produces more realistic moisture flux values leading to stronger boundary layer forcing for the initiation of deep convective initiation.

4.2 *28 June 2012 Houston, TX Case Study*

The 28 June 2012 case was selected to represent a typical, primarily sea-breeze driven, scattered convective coverage day. For forecasters, timing convective initiation and pinpointing the location of first initiates remains a difficult forecast problem. Warm season convective forecast uncertainty often results in a broad- brush forecast approach with a chance of showers and thunderstorms across the forecast area. In the case at hand, most first generation convection initiated in the vicinity of the sea-breeze boundary during the early afternoon hours. When comparing the reflectivity forecast from both the OPL and CTL runs vs. the actual reflectivity (see Fig. 5), both model forecasts appear very similar concerning the degree of convective coverage and this coverage appears representative; however, the model convection is displaced southwest of the actual convection. A comparison of the 6 hour Stage IV precipitation accumulation to the model accumulated precipitation fields reveals that both the OPL and CTL runs are underestimating precipitation coverage during the afternoon hours (see Fig. 6). These observations indicate that model generated convection is not as long lived in reality; and therefore, we need to investigate how to extend model convective cell lifetimes in these weakly forced convective events in order to generate additional precipitation.

5. PRELIMINARY OBJECTIVE VERIFICATION

Figure 7 shows gridded verification for 41 case days from the NWS Mobile domain. The Heidke Skill Score and frequency biases are given for both the OPL and CTL. The verification is performed out to 24 h and is based on a 24 km grid block for the neighborhood and a threshold of ≥1 mm h^{-1}. A simple inspection reveals a poorer forecast by the OPL run (i.e., the one with the NASA data sets) when compared to the CTL throughout roughly the first 18 forecast hours (with the exception of three apparent random hours). Interestingly, from forecast hours 19-24, the trend reverses. Although not shown and verification results are yet to be fully completed, similar results were found for the HGX domain with an independent sampling of a few case days. A number of variables differ between the model configurations used in this study and those used in the studies cited in the Section 1, so it is unclear at this time why the SPoRT datasets have independently outperformed a model without these data in other controlled modeling experiments but do not in the present study when combined. More work is required to better understand these differences. In both domains, a trend existed in which both models under-forecasted precipitation. Almost a decade of past observations regarding how mesoscale models handle convective initiation by the land-breeze over water areas during the early morning hours has not been encouraging. The authors strongly suspect that verification over 'land areas' only and after the land- and sea-breeze reversal will be more revealing.

6. SUMMARY AND FUTURE WORK

Current results are very preliminary and more work needs to be done especially with regard to determining how to best carry out the most effective and meaningful objective verification. There are current plans to perform verification over 'land only' areas during a time shortly after when the land- and sea-breeze circulations have reversed to better isolate and focus in on any potential impacts the GVF and LIS data sets may bring about. Furthermore, we intend to stratify the 'land only' verification by 0-1 km wind flow regime to examine any differences between the operational and control runs by a particular wind flow regime. As our primary concern is primarily on first initiates versus those of the second and third generations, we plan to also very closely examine the first hour either the operational, control and/or both models initiate deep convection. It is hoped after doing this more insight will be gained into the actual patterns of boundary layer moisture flux convergence, both sensible and latent heat fluxes and soil moisture, for example, which each help to collectively determine the observed pattern of first deep convective initiates versus where one might expect it to occur from analyzing model results. Finally, and depending upon the outcome of the latter verification results, additional model runs will be performed to optimize both the microphysics and boundary layer mixing schemes to see if it possible to eliminate the under-forecasted precipitation bias that occurs in both experiments.

7. REFERENCES

Brown, B. G., J. H. Gotway, R. Bullock, E. Gilleland, T. Fowler, D. Ahijevych, and T. Jensen, 2009: The Model Evaluation Tools (MET): Community tools for forecast evaluation. Preprints, *25th Conf. on International Interactive Information and Processing Systems (IIPS) for Meteorology, Oceanography, and Hydrology*, Phoenix, AZ, Amer. Meteor. Soc., 9A.6. [Available online at http://ams.confex.com/ams/pdfpapers/151349.pdf]

Case, J. L., W. L. Crosson, S. V. Kumar, W. M. Lapenta, and C. D. Peters-Lidard, 2008: Impacts of high-resolution land surface initialization on regional sensible weather forecasts from the WRF model. *J. Hydrometeor.,* **9,** 1249-1266.

Case, J. L., S. V. Kumar, J. Srikishen, and G. J. Jedlovec, 2011: Improving numerical weather predictions of summertime precipitation over the southeastern United States through a high resolution initialization of the surface state. *Wea. Forecasting,* **26,** 785-807.

Case. J. L., F. J. LaFontaine, S. V. Kumar, and C. D. Peters-Lidard, 2012: Using the NASA-Unified WRF to assess the impacts of real-time vegetation on simulations of severe weather. Preprints, *13th Annual WRF Users' Workshop,* P69. [Available online at https://www.regonline.com/AttendeeDocuments/1077122/43418383/43418383_1045166.pdf]

Kain, J. S., S. R. Dembek, S. J. Weiss, J. L. Case, J. J. Levit, and R. A. Sobash, 2010: Extracting unique information from high resolution forecast models: Monitoring selected fields and phenomena every time step. *Wea. Forecasting,* **25**, 1536-1542.

LaCasse, K. M., M. E. Splitt, S. M. Lazarus, and W. M. Lapenta, 2008: The impact of high-resolution sea surface temperatures on the simulated nocturnal Florida marine boundary layer. *Mon. Wea. Rev.,* **136,** 1349–1372.

Rozumalski, R. A., 2012: NEWR EMS User Guide. NOAA/NWS Forecast Decision Training Branch, COMET/UCAR. [Available on-line at http://strc.comet.ucar.edu/software/newrems/]

Skamarock, W. C., J. B. Klemp, J. Dudhia, D. O. Gill, D. M. Barker, M. G. Duda, X-Y. Huang, W. Wang and J. G. Powers, 2008: A Description of the Advanced Research WRF Version 3, NCAR Technical Note, NCAR/TN–475+STR, 123 pp. [Available on-line at http://www.mmm.ucar.edu/wrf/users/docs/arw_v3.pdf]

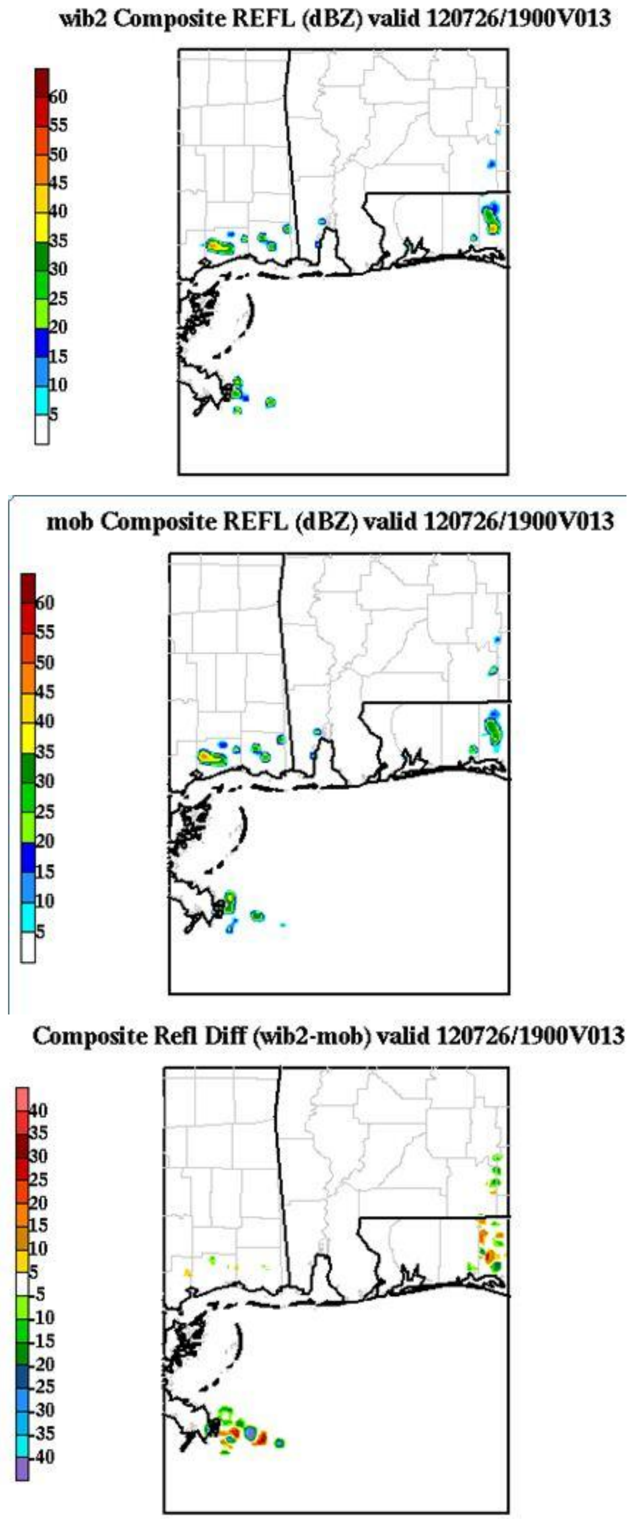

Figure 1. 13-h simulated radar reflectivity forecast showing evidence of non-linear variations that arise due to computational platform differences. Identical model runs performed at NASA SPoRT ('wib2', top) and NWS Mobile, AL ('mob', middle). The difference field is shown in the bottom image.

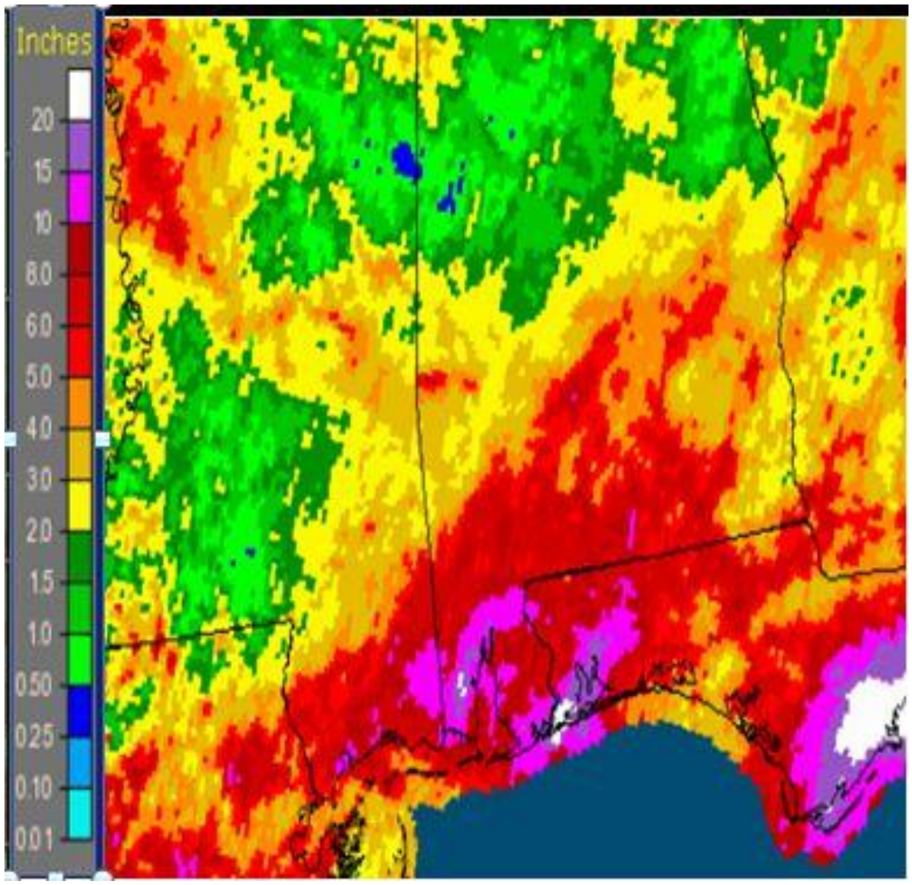

Figure 2. WSR-88D estimated rainfall for June 2012. Most of the rain fell along the Alabama and western Florida Panhandle coastlines during a three day period the first week of June.

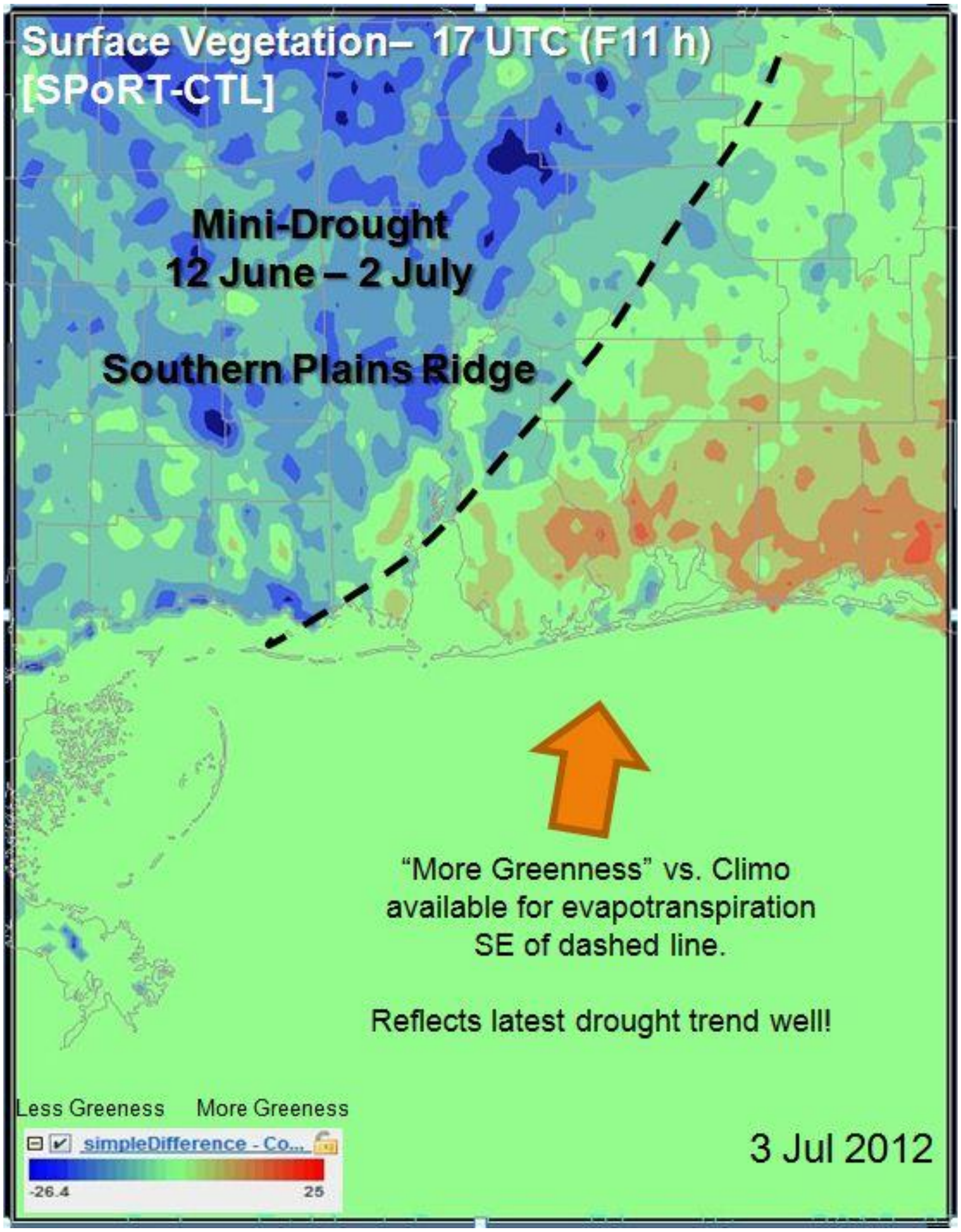

Figure 3. Difference field (OPL-CTL) for surface vegetation showing more 'greenness' vs. climatology along the Alabama and western Florida Coastal Zones. The effects of a 'mini-drought' are easily seen from southeastern MS and further northwestward.

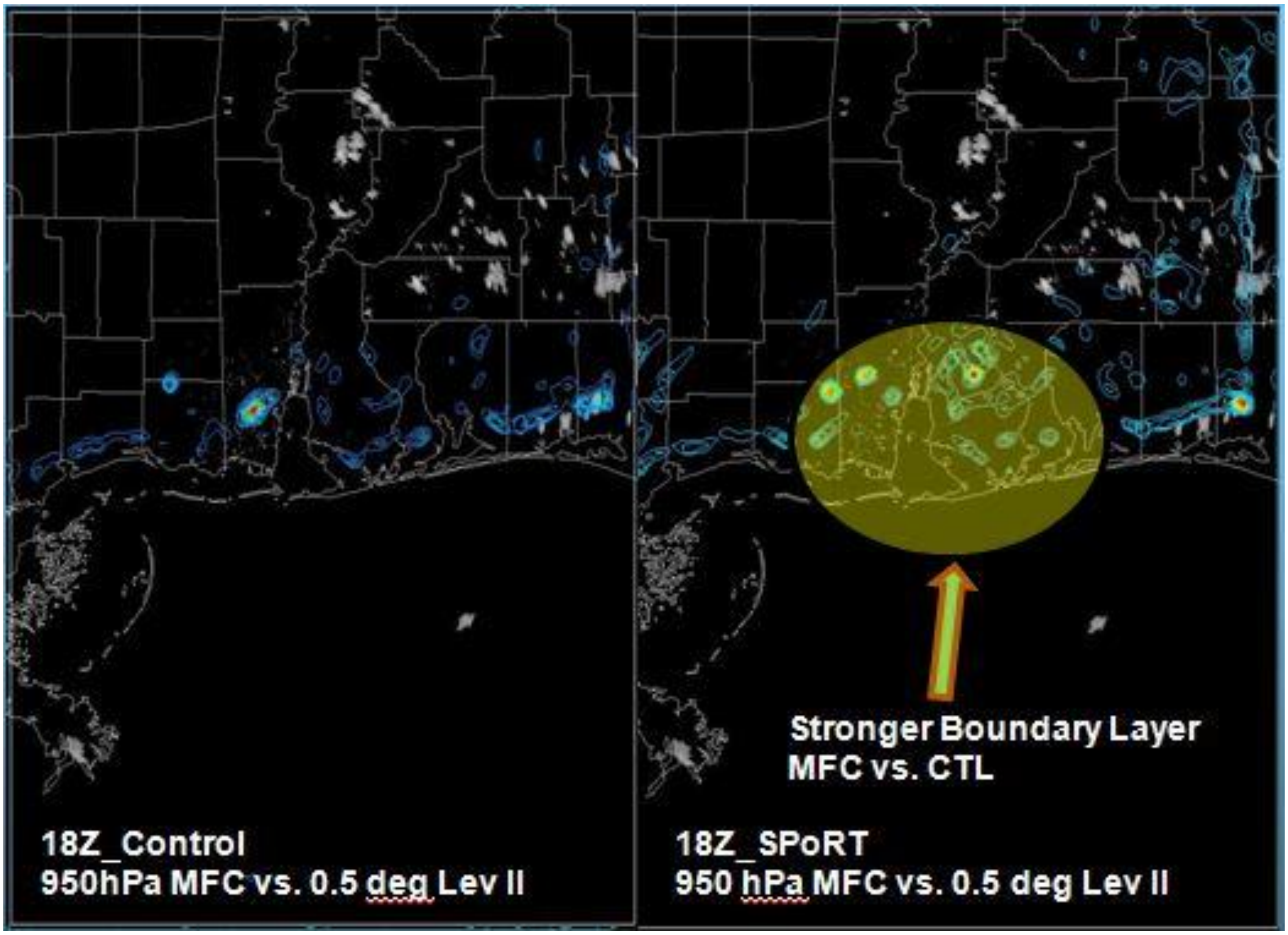

Figure 4. **12-h forecast 950 hPa moisture flux divergence (negative values only with blue contours and shading) forecast valid 18 UTC 3 July 2012 for the CTL (left) versus OPL (right). Radar reflectivity values ≥35 dBZ are in grey and are valid 1800 UTC. This is the closest time to when initiates first appeared along the coast. Note the relative stronger boundary layer moisture flux convergence along the Alabama and western Florida coastlines.**

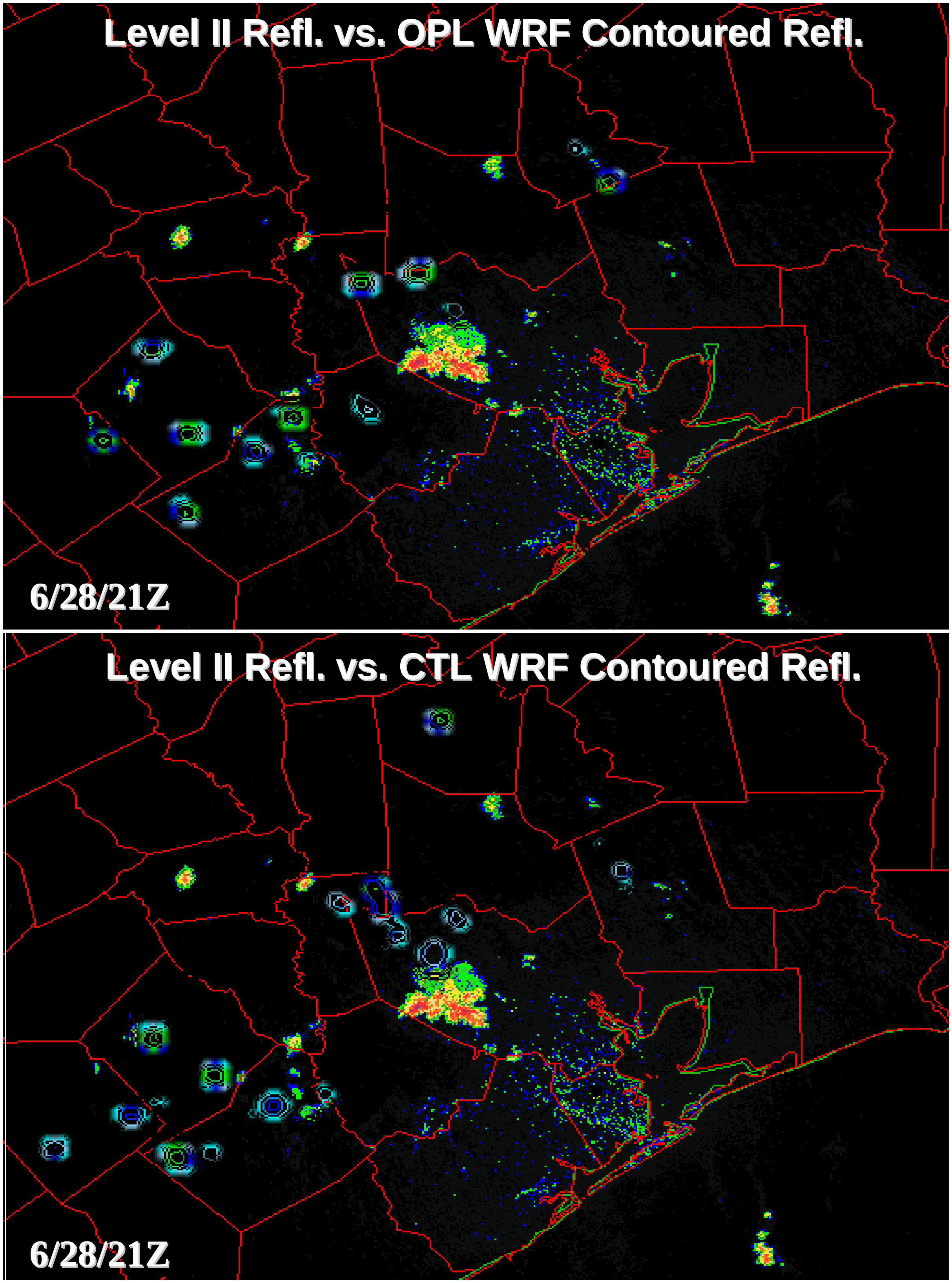

Figure 5. WSR-88D Level-II reflectivity vs. contoured WRF OPL (top) and CTL reflectivity (bottom) valid 21Z 28 June 2012.

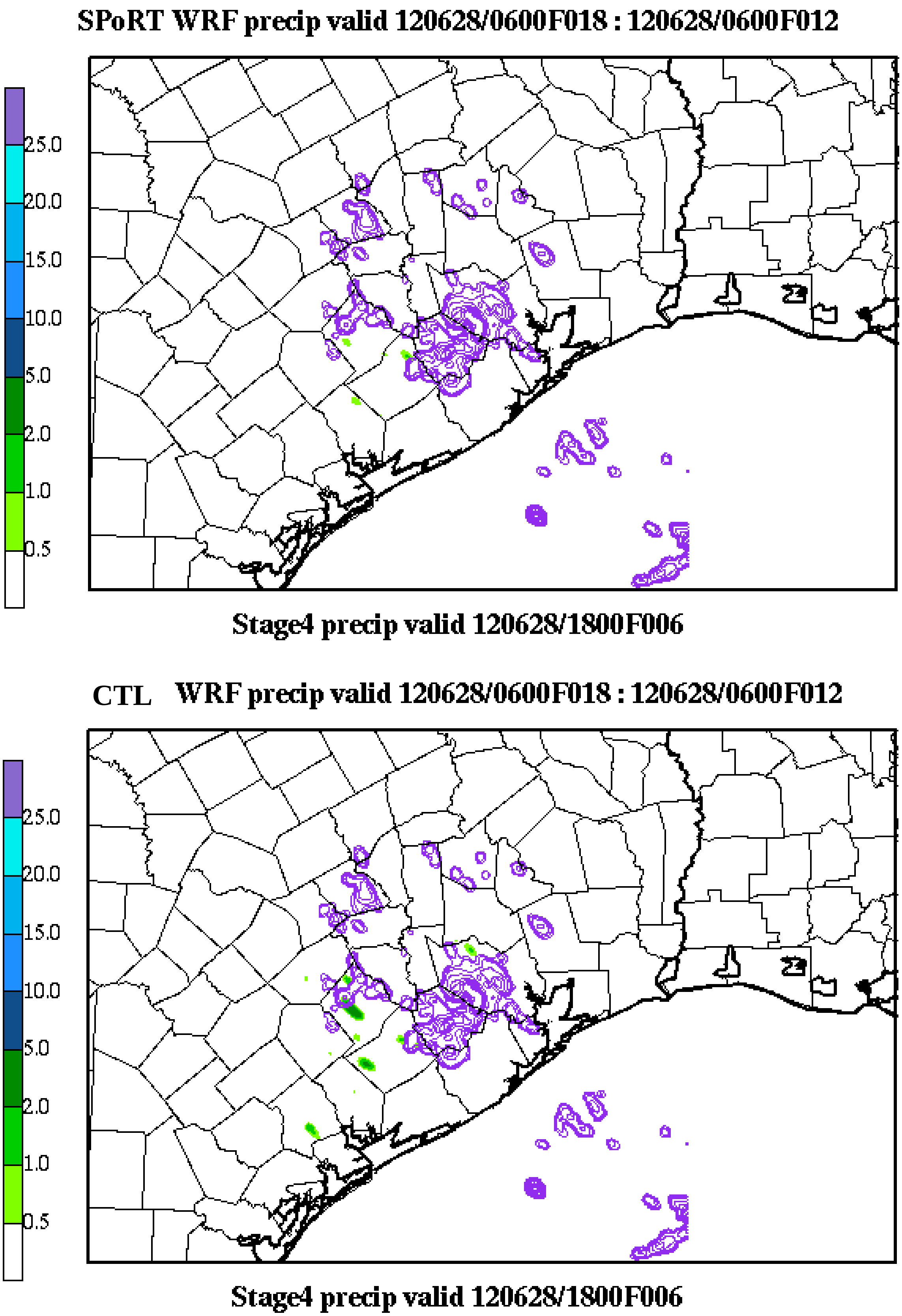

Figure 6. Stage IV Six Hour Accumulated Precip. vs. Contoured WRF Six hour Accumulated Precipitation OPL (top) and CTL (Bottom) valid from 18Z on June 28th 2012 to 00Z June 29th 2012.

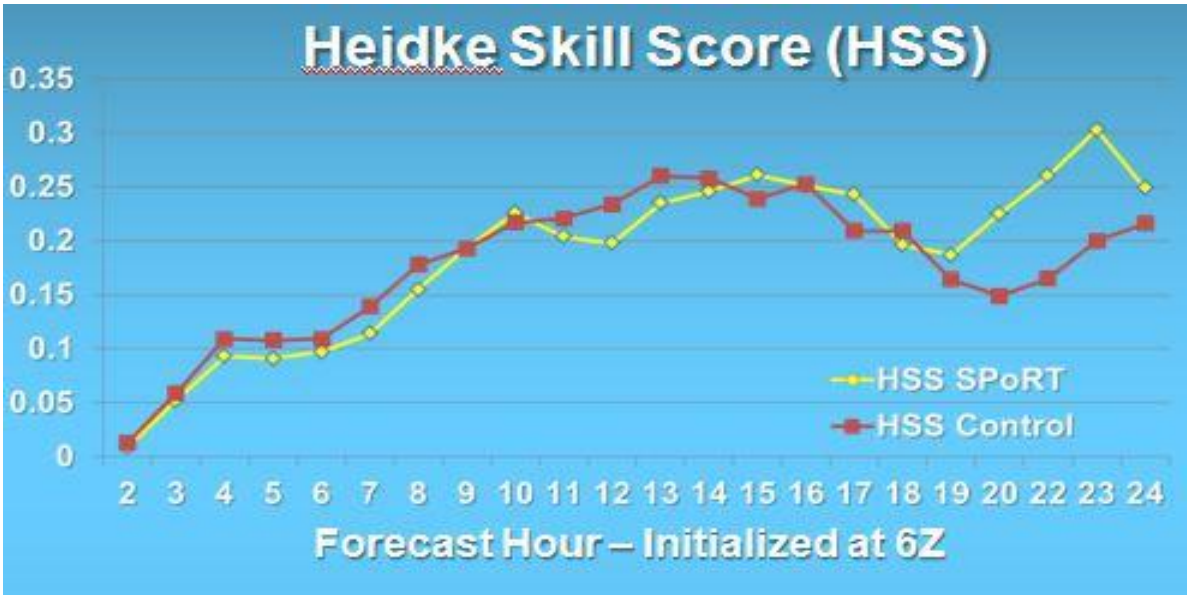

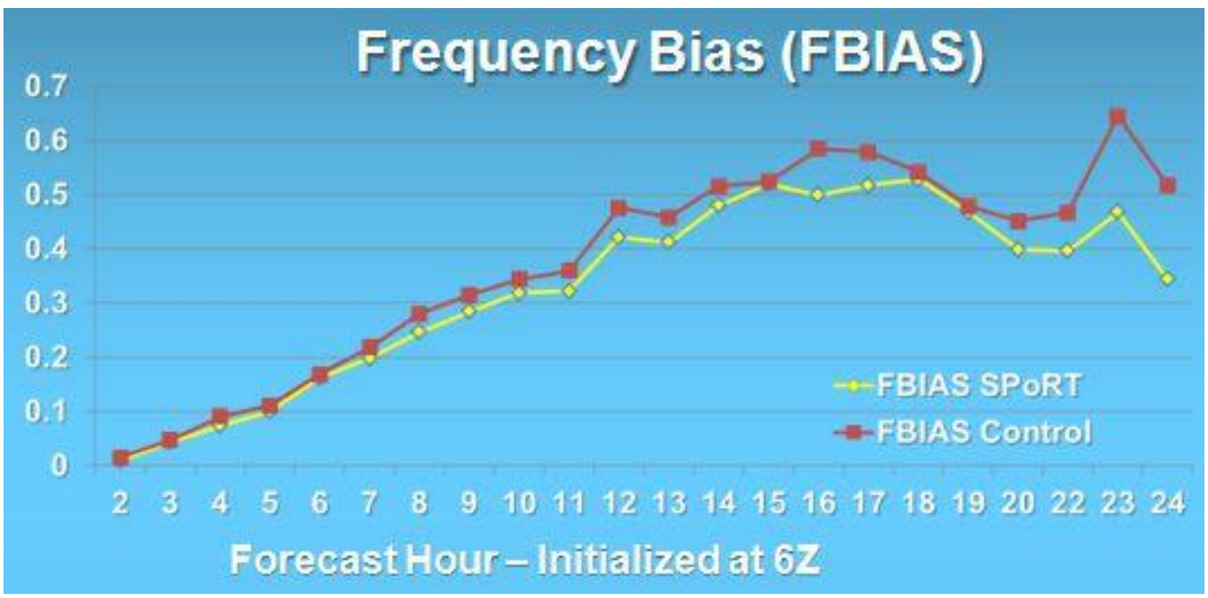

Figure 7. Heidke Skill Scores (HSS, top) and Frequency Biases (FBIAS, bottom) for all 41 OPL versus CTL runs verifying ≥1mm hourly accumulated model precipitation in MOB's domain out to 24 h beginning at 6 UTC. The verification is based on a 24 km grid block for the neighborhood and a threshold of ≥1 mm h^{-1}.